# CFD APPLIED TO SEPARATION OF SLAM-ER FROM THE S-3B

E. Ray
Member AIAA
Naval Air Systems Command
Patuxent River, MD

**Abstract**

The process of determining safe separation flight envelopes for release of the SLAM-ER missile from the S-3B platform is presented. Extensive use of Computational Fluid Dynamics (CFD) was employed in lieu of wind tunnel testing. CFD solutions for the aircraft/store mutual interference flowfield were placed into a database for use by Six-Degree of Freedom (6-DOF) trajectory simulation software. Simulated trajectories were used to predict the minimum miss distance between the SLAM-ER and S-3B.

The flight test program allowed for comparison of actual trajectories with predictions. Because the CFD/6-DOF trajectories correlated well with flight test results, two of the five planned flight test points were eliminated.

**Nomenclature**

| | |
|---|---|
| ψ, PSI | Store yaw angle, positive nose right, deg |
| θ, THETA | Store pitch angle, positive nose up, deg |
| ϕ, PHI | Store roll angle, positive right wing down, deg |
| Δψ, DPSI | Store yaw, pitch, and roll relative to carriage |
| Δθ, DTHETA | |
| Δϕ, DPHI | |
| X | Store CG location relative to carriage, positive forward, ft |
| Y | Store CG location relative to carriage, positive right, looking forward, ft |
| Z | Store CG location relative to carriage, positive down, ft |
| M | Mach number |
| $C_l$ | Rolling moment coefficient, positive right wing down |
| $C_m$ | Pitching moment coefficient, positive nose up |
| $C_n$ | Yawing moment coefficient, positive nose right |
| $C_N$ | Normal force coefficient, positive up |
| $C_Y$ | Side force coefficient, positive right, looking forward along store centerline |
| α, Alpha | Angle of Attack, deg |
| AOA | Angle of Attack, deg |
| β, Beta | Sideslip angle, deg |
| 6-DOF | Six-Degree of Freedom |
| AEDC | Arnold Engineering Development Center |
| CAD | Computer Aided Design |
| CFD | Computational Fluid Dynamics |
| CG | Center of Gravity |
| CTS | Captive Trajectory System |
| NAVSEP | Navy Generalized Six-Degree of Freedom Separation Package |
| RATV | Recoverable Air Test Vehicle |
| SLAM-ER | Standoff Land Attack Missile - Expanded Response |

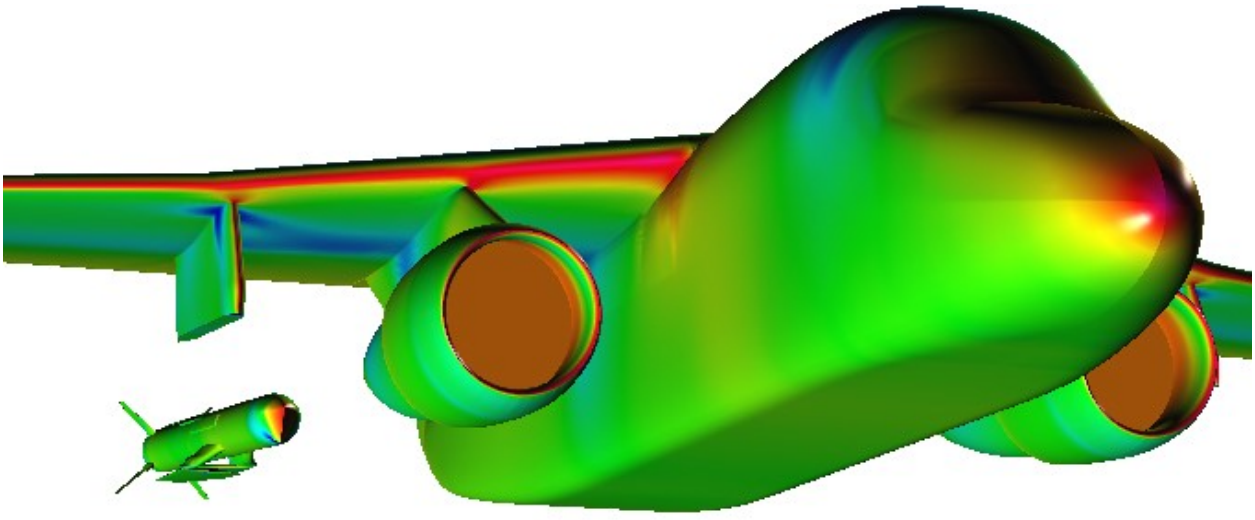

**Figure 1: S-3B and SLAM-ER Sample CFD Solution**

## Introduction

The U.S. Navy has developed an Integrated Test and Evaluation (T&E) approach to store separation which includes wind tunnel testing, simulation analysis, and ultimately flight tests.[1] The interaction between all three T&E components is essential for creating the arsenal for a new aircraft. However, when new stores are added to older platforms, the costs and lead times for wind tunnel testing can be prohibitive. The Navy has been tasked with upgrading the S-3B capabilities with the SLAM-ER (AGM-84H/K), an extended-range version of the Standoff Land Attack Missile (SLAM) shown in Figure 1. In order to make the program economically feasible, Computational Fluid Dynamics (CFD) has been used to take over the role generally given to wind tunnels, albeit in a limited fashion. This program was also a good candidate for CFD because a wind tunnel model of the S-3B was not available.

The S-3B is a carrier-based, high-wing aircraft used for Surface Warfare, Anti-Submarine Warfare, and Electronic Warfare. The S-3B is powered by twin General Electric TF34 high-bypass turbofan engines installed on wing pylons. The SLAM-ER is released from the external pylon on either wing outboard from the engine nacelle. Ejector cartridges provide forces to initiate the separation.

To date, the Navy Store Separation Branch has generally confined CFD to preliminary studies in support of extensive wind tunnel tests. Wind tunnel tests often begin with trajectories from Captive Trajectory System (CTS) rigs, which can be used to plan the more extensive aircraft/store mutual interference aerodynamic grids. Grid data, in addition to store freestream data, allow later trajectory simulations with Six Degree of Freedom (6-DOF) software. The ability to simulate large numbers of trajectories off-line is important for performing parametric studies for varieties of store mass properties, aircraft release conditions, ejector properties, etc.

## Methodology

While CFD has been used to create time-accurate trajectories similar to those of CTS testing[2], it was decided that an aircraft/store grid database created by CFD would be of much more utility. At current computing speeds, Euler methods could possibly provide as much data as wind tunnels, but of questionable quality. It was therefore decided that the viscous information was essential for this program, so use of the complete compressible Navier-Stokes equations would be needed.

For the project time frame, the number of quality CFD solutions would be much smaller than the number of data points available in a typical wind tunnel grid program, so it was necessary to make the most use out of the least number of CFD runs. Experience has tended to reduce the amount of data taken in the wind tunnel while still maintaining the ability to create reliable trajectory predictions. For example, grid surveys used to be done perpendicular to the wind tunnel axis regardless of the store released and the aircraft angle of attack, and often for more than one X and Y position. A better way is to use knowledge about the store, or even CTS runs, to perform grid surveys along paths that better reflect the expected store trajectories.[3]

For a typical wind tunnel grid run at a given Mach number, there might be 8 store DPSI and DTHETA combinations. A typical Z-sweep could have a maximum of approximately 21 positions, as shown in Figure 2. Z-sweeps with yaw and pitch would have to omit some locations that physically bring the store model too close to the aircraft model.

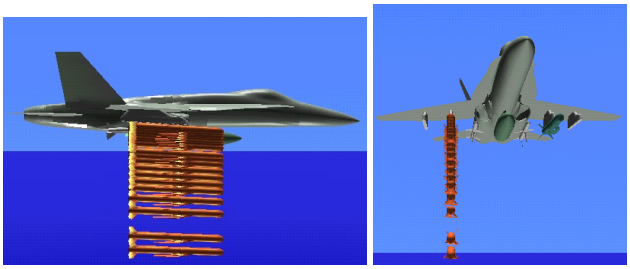

**Figure 2: Typical Wind Tunnel Grid Z-Sweep Approximately 21 Positions**

The minimum number of SLAM-ER positions thought necessary to determine a reliable database is shown in Figures 3 through 6.

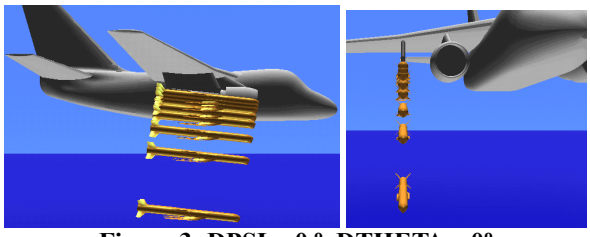

**Figure 3: DPSI = 0 º, DTHETA = 0º 8 Positions**

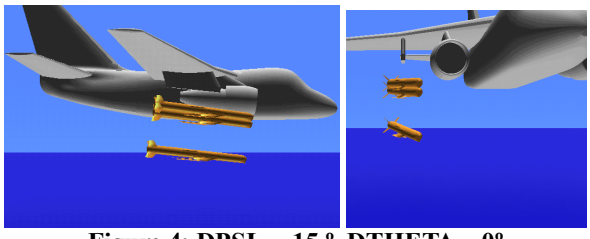

**Figure 4: DPSI = -15 º, DTHETA = 0º 3 Positions**

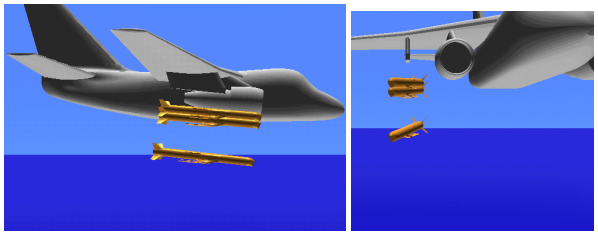

Figure 5: DPSI = +15 º, DTHETA = 0º
3 Positions

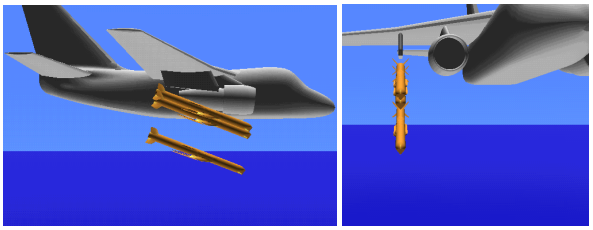

Figure 6: DPSI = 0 º, DTHETA = -15º
3 Positions

Table 1: Grid Matrix Comparison

| | | Typical Wind Tunnel Grid Matrix | | | | | | | | CFD Grid Matrix | | | |
|---|---|---|---|---|---|---|---|---|---|---|---|---|---|
| $Z_{REF}$ (ft) | $\Delta\psi$: | 0° | 0° | 0° | 0° | 10° | 10° | 10° | 20° | 0° | -15° | 15° | 0° |
| | $\Delta\theta$: | 0° | -10° | -20° | -30° | -10° | -20° | -30° | -20° | 0° | 0° | 0° | -15° |
| 0.0 | | X | | | | | | | | X | | | |
| 0.2 | | X | | | | | | | | | | | |
| 0.5 | | X | | | | | | | | X | | | |
| 0.8 | | X | | | | | | | | | | | |
| 1.0 | | X | X | | | | | | | X | | | |
| 1.3 | | X | X | | | X | | | | | | | |
| 1.7 | | X | X | | | X | | | | | | | |
| 2.0 | | X | X | | | X | X | | | X | X | X | X |
| 2.5 | | X | X | | | X | X | | | | | | |
| 3.0 | | X | X | X | | X | X | | | X | X | X | X |
| 3.7 | | X | X | X | | X | X | | | | | | |
| 4.3 | | X | X | X | X | X | X | | X | | | | |
| 5.0 | | X | X | X | X | X | X | X | X | X | | | |
| 6.0 | | X | X | X | X | X | X | X | X | | | | |
| 7.0 | | X | X | X | X | X | X | X | X | | | | |
| 8.0 | | X | X | X | X | X | X | X | X | X | X | X | X |
| 9.0 | | X | X | X | X | X | X | X | X | | | | |
| 10.5 | | X | X | X | X | X | X | X | X | | | | |
| 12.3 | | X | X | X | X | X | X | X | X | | | | |
| 16.0 | | X | X | X | X | X | X | X | X | X | | | |
| 18.0 | | X | X | X | X | X | X | X | X | | | | |
| | | 109 Data Points | | | | | | | | 17 Data Points | | | |

A typical wind tunnel run might take data at approximately 109 store placements multiplied by a range of about 3 aircraft Angles of Attack, leading to over 300 data points. Using *a priori* knowledge of the S-3B, the number of data points are reduced by performing all CFD at the actual aircraft Angle of Attack at release. Therefore approximately 17 CFD solutions would be required for a given flight condition. Typical wind tunnel and CFD grid matricies are compared in Table 1.

The structured overset grid or "chimera" technique, introduced by Steger *et al.*[4] and Benek *et al.*[5], seemed the ideal method for rapid grid generation for the store in several positions under the parent aircraft. The preprocessing or "hole cutting" of grids was performed using the PEGSUS software.[6] Due to its relatively fast performance, OVERFLOW was the employed flow solver.[7] OVERFLOW solves the compressible Navier-Stokes equations using finite differences in space and implicit time-stepping. All solutions were run with the grids fully viscous using the 1-equation Spalart-Allmaras $R_T$ turbulence model.[8] Once a CFD solution was obtained, force and moment coefficients for the SLAM-ER were calculated with the FOMOCO utility.[9]

## SLAM-ER CFD Model

The most significant aerodynamic difference between the SLAM-ER and baseline SLAM is the addition of folding wings located in the store undercarriage. The SLAM-ER would be well away from the aircraft before wing deployment, so all the analysis was performed with the wings in their stowed position. The SLAM-ER CFD model was created based on Computer Aided Design (CAD) geometry and is composed 3 million grid points from 18 overlapping meshes.

In order to validate the SLAM-ER CFD model, isolated runs were conducted and compared to wind tunnel freestream data. Wind tunnel data were available from a 10% scale model at the Arnold Engineering Development Center (AEDC) 16T.[10] Additional data were taken from a 6% model at the Veridian (a.k.a. CALSPAN) 8-ft Transonic Wind Tunnel.[11] Figures 7 and 8 show the results of CFD freestream runs compared to wind tunnel AOA ($\alpha$) sweeps with a sideslip angle ($\beta$) of zero degrees for Mach numbers of 0.46 and 0.80. Because $\beta = 0$ degrees, only the pitching moment ($C_m$) and normal force ($C_N$) coefficients are shown.

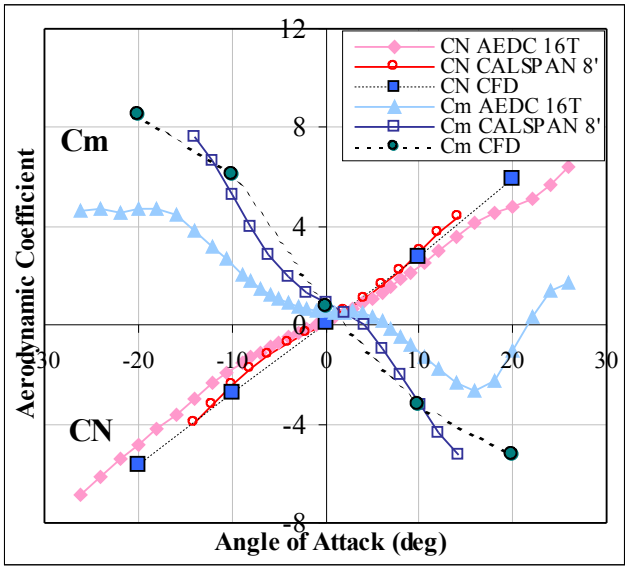


**Figure 7: SLAM-ER Freestream Comparison for M = 0.46, $\beta = 0°$**

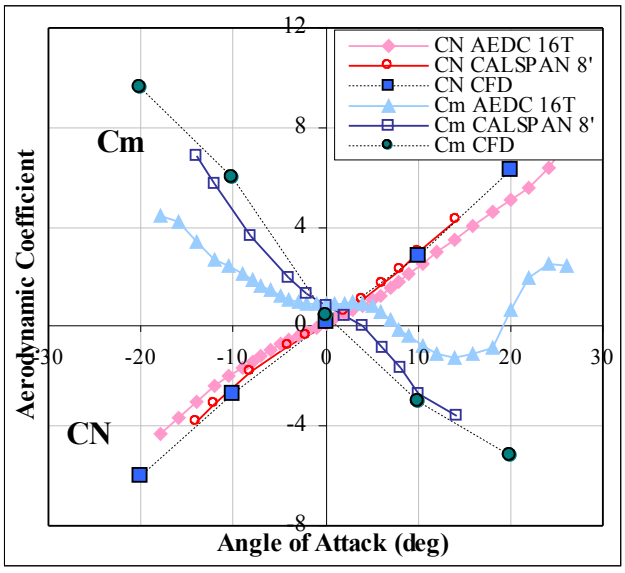


**Figure 8: SLAM-ER Freestream Comparison for M = 0.80, $\beta = 0°$**

One will note that the difference between results from the two wind tunnels is significant. Because AEDC 16T is a larger wind tunnel than CALSPAN 8-ft, in addition to using a larger-scale model, it is considered to be of higher accuracy. Nevertheless, the CFD data tend to agree more with the results from CALSPAN 8-ft.

Figures 9 and 10 show the comparison of sideslip sweeps with $\alpha = 0$ degrees at Mach numbers of 0.46 and 0.80. The side force ($C_Y$) and yawing moment ($C_n$) coefficients also have some disparity between wind tunnels, with the CFD results being closer to those of CALSPAN 8-ft.

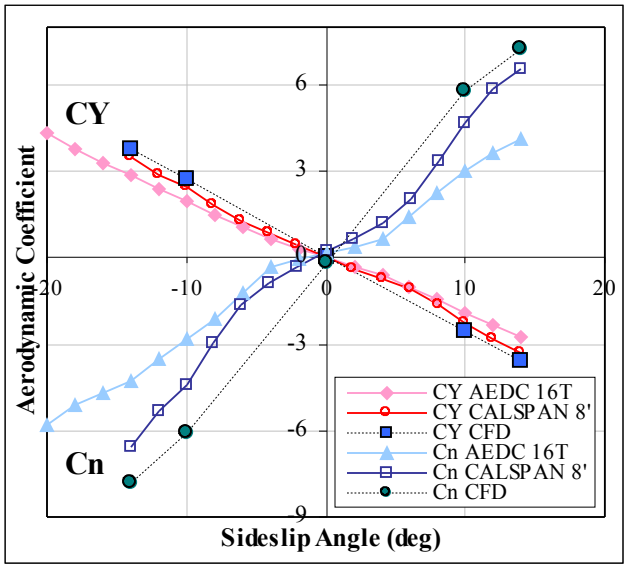


**Figure 9: SLAM-ER Freestream Comparison for M = 0.46, $\alpha = 0°$**

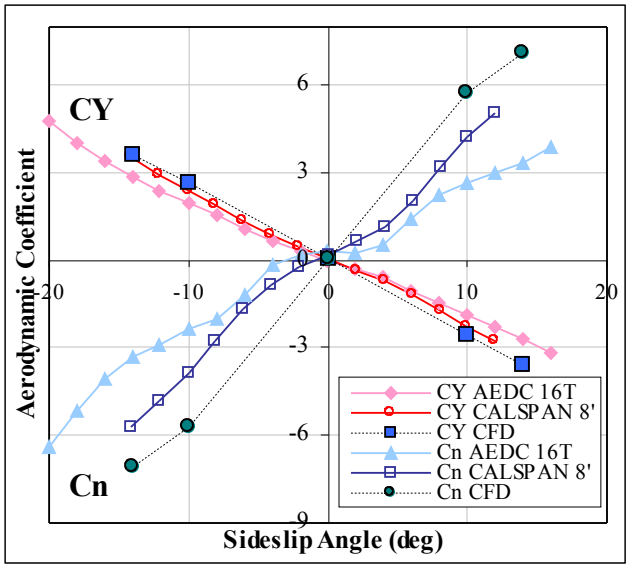


**Figure 10: SLAM-ER Freestream Comparison for M = 0.80, $\alpha = 0°$**

## S-3B CFD Model

The S-3B CFD model was generated from CAD geometry with 5 million grid points from 19 meshes. The combined S-3B/SLAM-ER grid (Figure 11) was approximately 8 million grid points, for which convergence was achieved between 2,500 and 3,500 iterations. Computations were performed at High Performance Computing sites on either SGI Origin or IBM SP2 supercomputers. Using 12 processors, a typical solution took 680 CPU hours for a total wall clock time of approximately 86 hours.

Because of the close proximity of the SLAM-ER to the S-3B engine nacelle, bypass flow had the potential to adversely affect separation performance. To account for this, a variety of engine boundary conditions had to be studied. Mass flow, stagnation temperature, and stagnation pressure boundary conditions were applied to the engine inlet, bypass flow exit, and core engine exit. CFD solutions were obtained for the SLAM-ER at carriage position for three engine throttle settings: flight idle, standard power, and full power. The engine setting that resulted in the largest carriage moments was then used for the rest of the CFD calculations for the given flight condition.

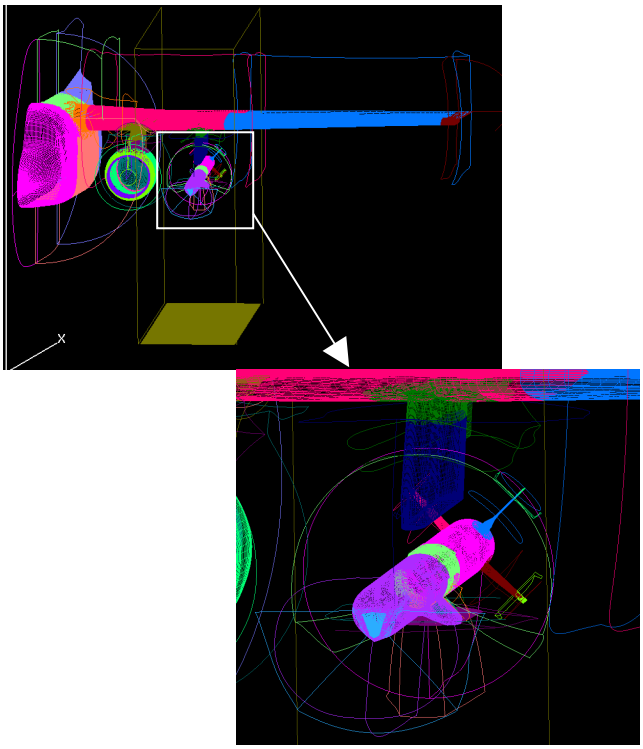

**Figure 11: S-3B and SLAM-ER CFD Models**

## S-3B Simulation Comparison With Flight Testing

To determine the safe S-3B/SLAM-ER release envelope, a flight test program was originally planned with five release events. The first event would be in the center of the release envelope, where separation was expected to be safe. Before moving to the high-speed release point, an intermediate release was planned. Similarly, a build-up point was planned before the low-speed release point. CFD/6-DOF trajectory predictions were performed at these same flight conditions. Over the course of the program, such confidence was gained in the analytical model that the two intermediate flight test points were eliminated.

Trajectories were predicted using the CFD-derived aerodynamic database and SLAM-ER freestream data from the CALSPAN 8-ft wind tunnel with the 6-DOF NAVSEP trajectory simulation code. A wide-range of parametric studies were conducted for varying store mass properties, flowfield intensity, and ejector forces.

Following safe separation predictions, flight testing was performed with a Recoverable Air Test Vehicle (RATV) which simulates the shape and mass properties of the AGM-84H/K (SLAM-ER) and was equipped with a telemetry package for flight data acquisition. Each RATV was equipped with a parachute to allow for its recovery. The S-3B test aircraft was instrumented with cameras, allowing photogrammetric trajectory data. After each flight event, the NAVSEP simulation code was again used to calculate trajectories using the exact measured Mach number, altitude, and flight path angle at store release.

The first SLAM-ER separation from the S-3B involved straight and level release at a Mach Number of 0.59 at an altitude of 6,940 feet with an aircraft AOA of 2.3°. The first separation trajectory displacements and attitudes for the first 400 milliseconds after release are plotted in Figures 12 through 17. The simulated trajectory agrees well with flight test telemetry and photogrammetric data. Note that the data points presented for all trajectories represent only a sampling of the available data for illustrative purposes.

The worst case engine setting for this Mach Number was determined to be full power, so CFD analysis at this was conducted with the corresponding boundary conditions. This is probably the reason that the simulated yaw (Figure 15) and pitch (Figure 16) are greater than that experienced in flight. The simulation was not expected to simulate roll as well (Figure 17) because off-axis ejector forces can cause unpredictable roll rates.[12]

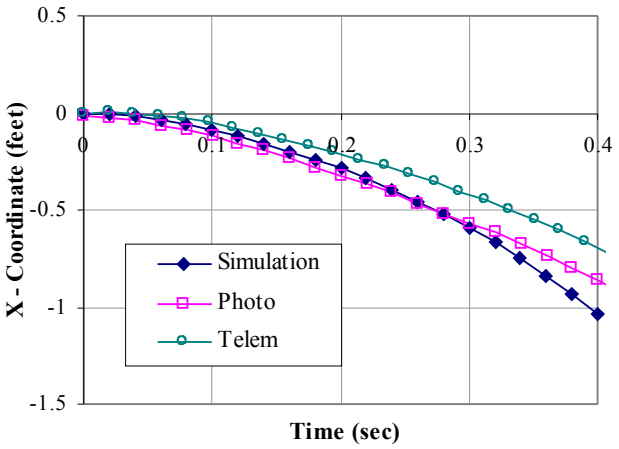


Figure 12: Flight Test 1 Longitudinal Displacement

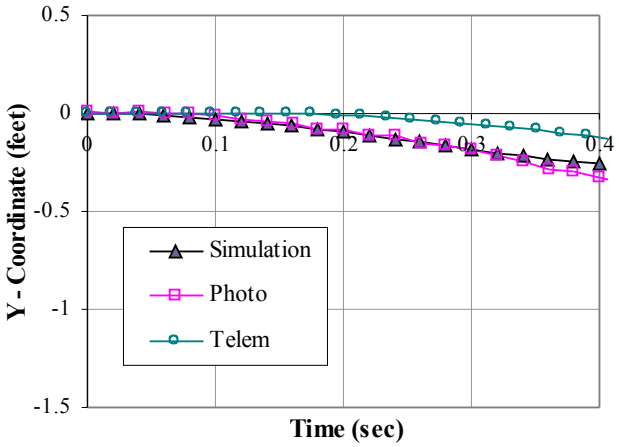


Figure 13: Flight Test 1 Lateral Displacement

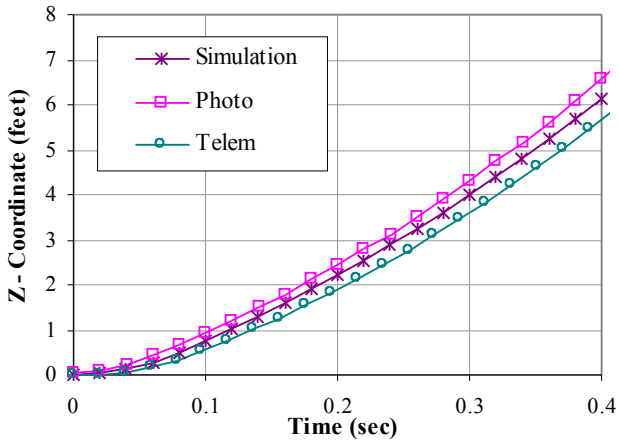


Figure 14: Flight Test 1 Vertical Displacement

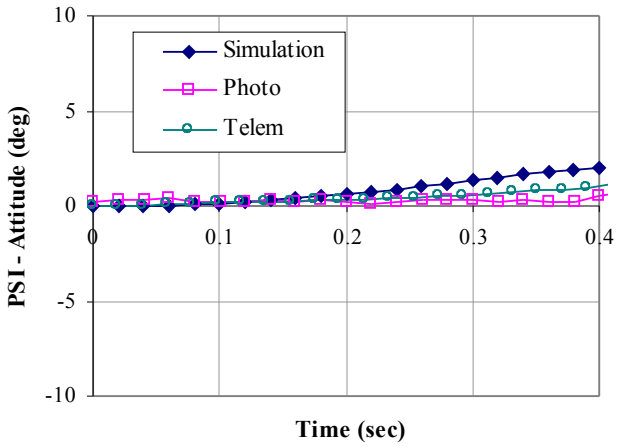


Figure 15: Flight Test 1 Yaw Attitude

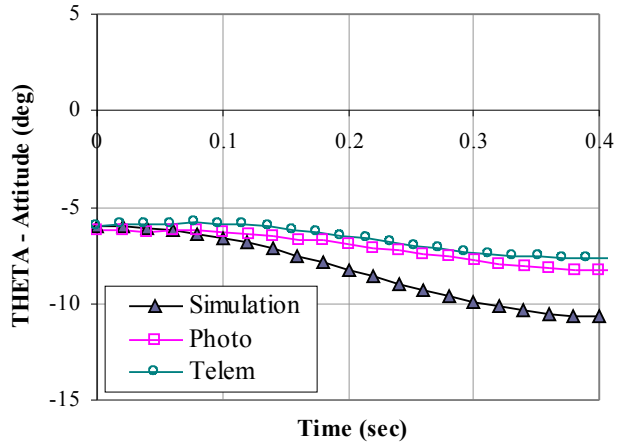


Figure 16: Flight Test 1 Pitch Attitude

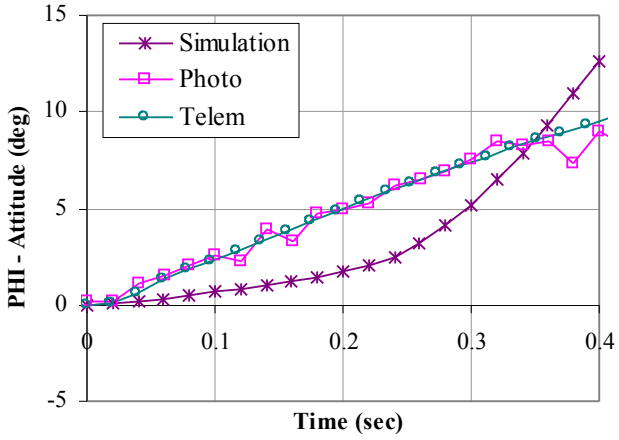


Figure 17: Flight Test 1 Roll Attitude

Given data on the store position and attitude, as well as geometry models, it was possible to compute miss distances. The miss distance code used modified PLOT3D CFD models. To speed up computation, the models used were of less fidelity than those used for CFD. Care was taken to minimize error by leaving in critical features of the models (corners, etc.). In the case of photogrammetrics, it is possible to determine miss distances directly from the images. However, it was decided to indirectly use the photogrammetric data to determine positions and attitudes for input into the miss distance code, in keeping with the other data sources.

Previous flight test experience has shown that photogrammetrics tends to measure store displacement better than telemetry because the inertial acceleration of the store will not account for the relative displacement of the pylon due to aircraft roll and wing flexure. However, telemetry does generally provide better store attitude data than photogrammetrics because of limitations in camera placement. Therefore, a composite miss distance was also calculated comprised of displacement from photogrammetrics and attitudes from telemetry, which should best reflect the "truth" of the flight test. A comparison of these miss distance histories between the SLAM-ER and S-3B pylon is presented in Figure 18. The simulated miss distance is bounded by those obtained from telemetry and photogrammetrics, leading to confidence in the CFD/6-DOF model.

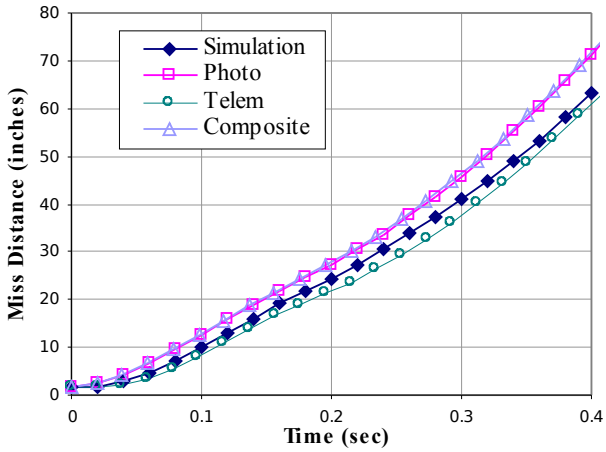


**Figure 18: Flight Test 1 Miss Distance**

Because the simulations for the high-speed end of the flight envelope predicted safe separations, and because of the good correlation with the first flight event, the second flight test was conducted at the high-speed test point, rather than at an intermediate point. The release conditions were Mach 0.70, approximately 7,000 ft altitude and an aircraft AOA of 2.1°. The simulated trajectory is compared with flight test data in Figures 19 through 24. While CFD was conducted at the worst case throttle setting of flight idle, the actual flight was most likely performed at a higher engine setting, leading to differences in the trajectory. The carriage yawing moment, for example, was a factor of 4.5 greater at flight idle than at standard power. As expected, the simulated trajectory was therefore overly conservative, notably in X-displacement (Figure 19), yaw (Figure 22), and pitch (Figure 23). In addition, the high dynamic pressure might have led to pockets of transonic flow, which CFD can have some difficulty predicting.

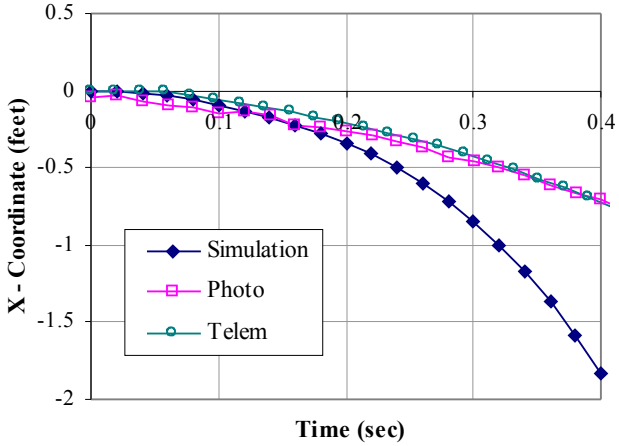


**Figure 19: Flight Test 2 Longitudinal Displacement**

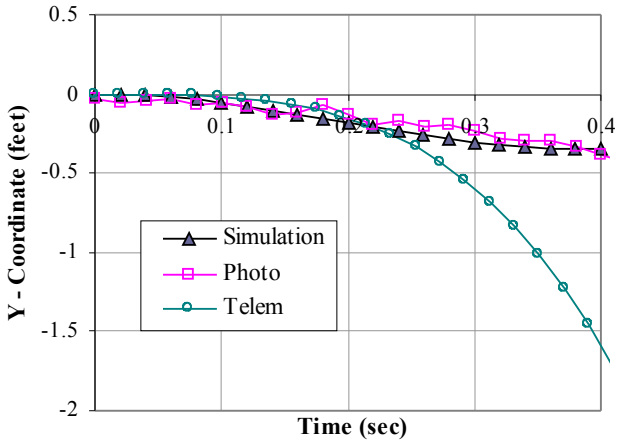


**Figure 20: Flight Test 2 Lateral Displacement**

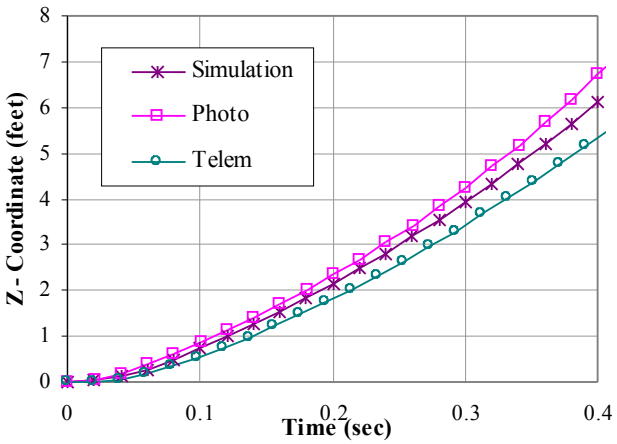


**Figure 21: Flight Test 2 Vertical Displacement**

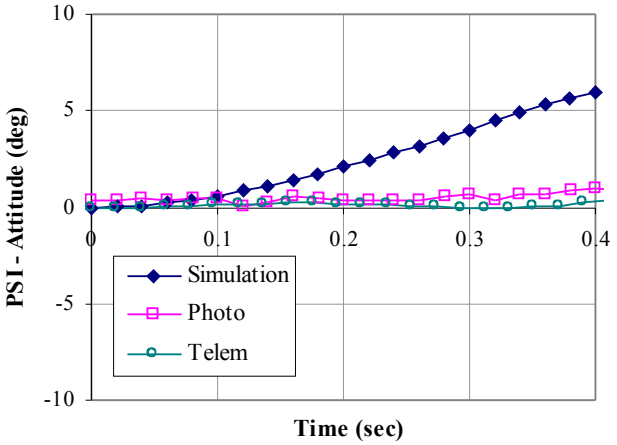


**Figure 22: Flight Test 2 Yaw Attitude**

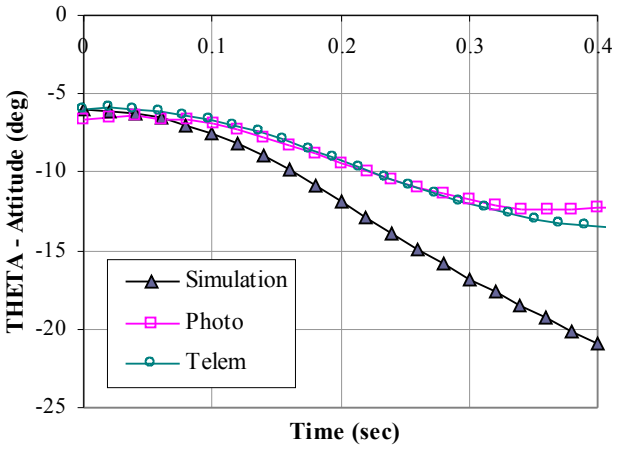


**Figure 23: Flight Test 2 Pitch Attitude**

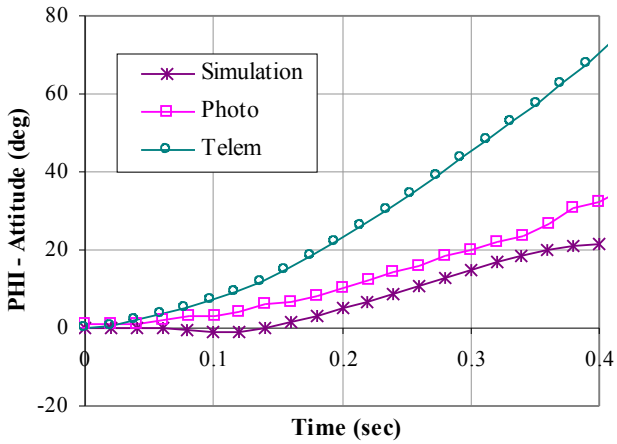


**Figure 24: Flight Test 2 Roll Attitude**

Despite the differences in the trajectory, the miss distance predictions were similar to those from flight test. The composite "truth" miss distance agrees well with the simulation up until about 250 milliseconds, after which the simulated miss distance is more conservative.

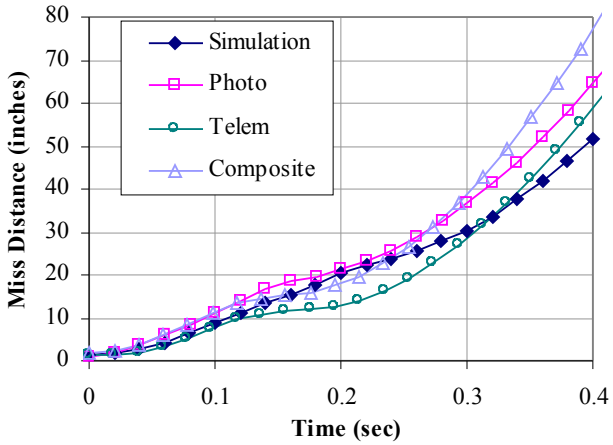


**Figure 25: Flight Test 2 Miss Distance**

Simulations for the low-speed end of the release envelope predicted safe separation for the SLAM-ER from the S-3B. Because the predictions from CFD up to this point had been accurate and/or conservative, the third flight test was conducted at the low-speed end of the envelope rather than the planned build-up point. This condition was Mach 0.45, approximately 7,500 ft altitude and 4.4° aircraft AOA. As predicted, the trajectory at this condition was benign (Figures 26 through 31) and correlation was exceptionally good. CFD was conducted at the worst case throttle setting of flight idle, which was likely close to reality.

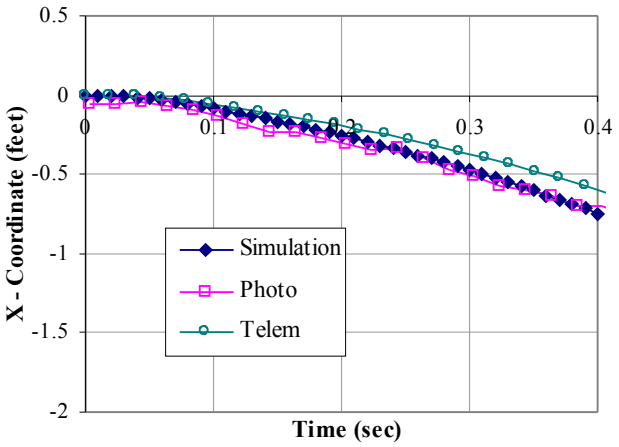


Figure 26: Flight Test 3 Longitudinal Displacement

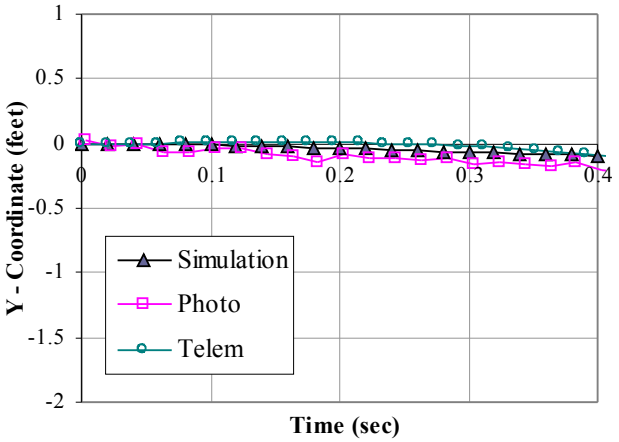


Figure 27: Flight Test 3 Lateral Displacement

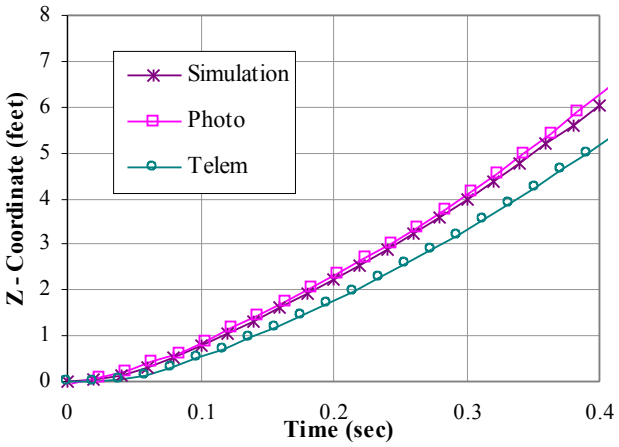


Figure 28: Flight Test 3 Vertical Displacement

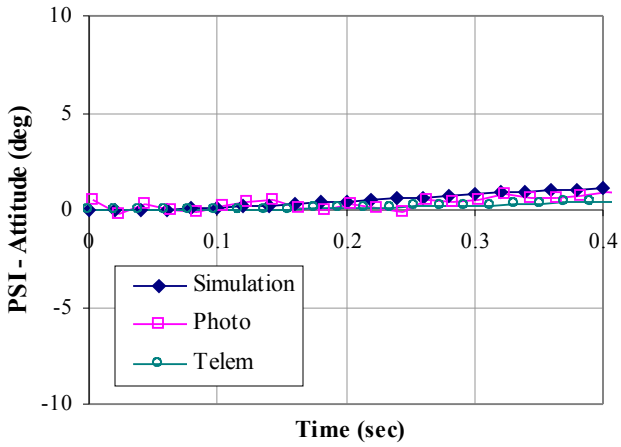


Figure 29: Flight Test 3 Yaw Attitude

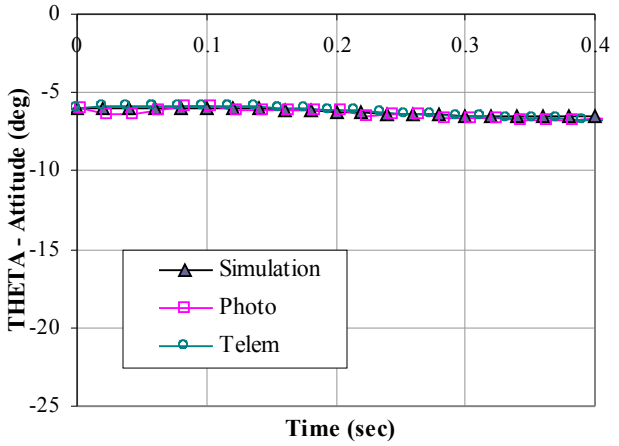


Figure 30: Flight Test 3 Pitch Attitude

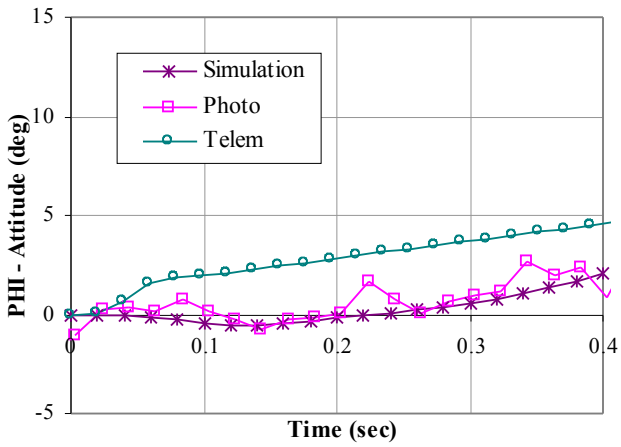


Figure 31: Flight Test 3 Roll Attitude

In all flight tests, telemetry tended to show a questionably low Z-displacement, which tended to lead to a smaller miss distance. Again, the simulated miss distance for this flight (Figure 32) agrees quite well with that of the composite photogrammetric/telemetry trajectory.

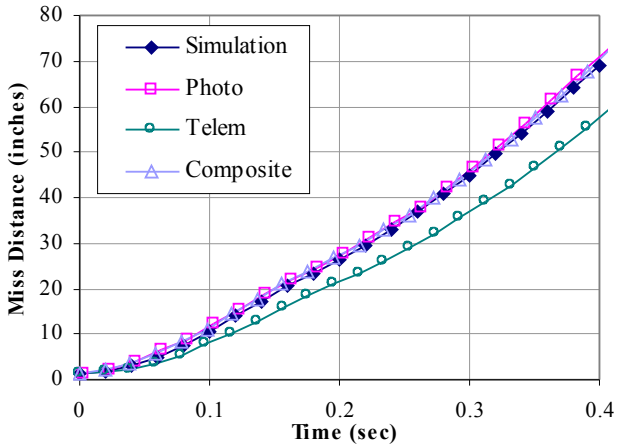


**Figure 32: Flight Test 3 Miss Distance**

## Conclusion

CFD was used successfully to provide a flight release envelope for the SLAM-ER from the S-3B. The first step for validation of the CFD model was comparing existing wind tunnel freestream data with isolated SLAM-ER CFD solutions. CFD results tended to agree generally with the wind tunnel database.

CFD data were then input into the NAVSEP separation simulation, in a similar manner to the wind tunnel grid method. Predicted trajectories, and ultimately miss distances between the SLAM-ER and the S-3B, agreed well with flight test results, leading to great confidence in the model and procedure. This analytical capability allowed for the elimination of two of the five planned flight tests, resulting in considerable cost savings.

This method is currently being applied to clear the SLAM-ER from the P-3C maritime patrol aircraft. This effort is more difficult because there are more possible loading configurations, many involving adjacent stores. A paper describing this project will follow the completion of the corresponding integration effort.

## References

1. Taverna, F. P., Cenko, A., "Navy Integrated T&E Approach to Store Separation," Paper 13, RTO Symposium on Aircraft Weapon System Compatibility and Integration, Chester, UK, October 1998.

2. Sickles, W. L., Denny, A.G., Nichols, R. H., "Time-Accurate CFD Predictions of the JDAM Separation from an F-18C Aircraft," AIAA Paper 2000-0796, January 10-13, 2000.

3. Krekeler, G. C., Popham, E. R., Chaddock, D. R., "F/A-18E/F Weapons Separation Program," AIAA Paper 99-0394, January 1999.

4. Steger, J. L., Dougherty, F. C., Benek, J. A., "A Chimera Grid Scheme," ASME Mini-Symposium on Advances in Grid Generation, 1982.

5. Benek, J. A., Buning, P. G., Steger, J. L., "A 3-D Chimera Grid Embedding Technique," AIAA Paper 85-1523, 1985.

6. Suhs, N. E., Tramel, R.W., "PEGSUS 4.0 User's Manual," AEDC-TR-91-8, November 1991.

7. Buning, P.G., "OVERFLOW User's Manual," February 1999.

8. Spalart, P. R., Allmaras, S. R., "A One Equation Turbulence Model for Aerodynamic Flows," AIAA Paper 92-0439, January 1992.

9. Chan, W. M., Buning, P. G., "User's Guide for FOMOCO Utilities – Force and Moment Computation Tools for Overset Grids," NASA TM 110408, July 1996.

10. Veazey, D. T., Hopf, J. C., "Comparison of Aerodynamic Data Obtained in the Arnold Engineering Development Center Wind Tunnels 4T and 16T," AIAA, 1998.

11. Felder, B., *et al*. "Upgrading the Weapons Integration Testing Capabilities at Calspan's Transonic Wind Tunnel Facility," Prepared for 89th Semi-Annual Meeting of the Supersonic Tunnel Association International, April 1998.

12. Cenko, A., "F/A-18C/JDAM CFD Challenge Wind Tunnel and Flight Test Results," AIAA Paper 99-0120, January 1999.